Reactions of Laser-Ablated Palladium and Platinum Atoms with Nitric Oxide: Infrared Spectra and Density Functional Calculations of $MNO^{+,0,-}$ and $M(NO)_2$ in Solid Argon and Neon

Angelo Citra and Lester Andrews*

Department of Chemistry, University of Virginia, Charlottesville, Virginia 22904-4319

Received: March 1, 2000; In Final Form: June 20, 2000

Laser-ablated palladium and platinum atoms react with NO in excess argon or neon to form $Pd(NO)_{1,2}$ and $Pt(NO)_{1,2}$ as major products. DFT calculations are found to be effective in reproducing experimental results and in assigning observed bands. Nitrosyl cation and anion species are observed with both metals, and a linear relationship is found between the charge and nitrosyl stretching frequencies in $Pd(NO)^{+,0,-}$ and $Pt(NO)^{+,0,-}$ that allows estimates of charges on supported Pt and Pd catalysts to be made.

Introduction

Considerable experimental and theoretical work has been performed on the palladium and platinum dimers, trimers, and larger clusters, due to the importance of supported platinum metal catalysts in controlling the emission of nitrogen oxides.[1−9] The nitric oxide molecule has been studied on the metal surfaces, and the chemisorption behavior is found to be more complex than that for carbon monoxide due to the extra electron and more favorable energy matching with the metal d-levels.[10−13]

Following extensive investigations of laser-ablated transition metal reactions with nitric oxide in this laboratory,[14−21] laser-ablated palladium and platinum atoms are reacted with nitric oxide and products are isolated in argon and neon matrices. Mononuclear, binuclear, cation and anion nitrosyl species are observed for both metals, and the N−O stretching frequencies for these species are found to correlate well with those observed for nitric oxide in different sites on the metal surfaces. Similar neutral and charged species have been produced in analogous laser-ablation experiments with iron, cobalt, and nickel,[18] and neutral nitrosyls have been formed in earlier thermal metal atom investigations.[22,23] Density functional theory (DFT) isotopic frequency calculations are found to reproduce the experimental results to a comparable degree of accuracy for several different products. The BPW91 and B3LYP functionals provide complimentary results that aid in assigning the observed bands.

Experimental Section

The experiment for laser ablation and matrix isolation has been described in detail previously.[24,25] Briefly, the Nd:YAG laser fundamental (1064 nm, 10 Hz repetition rate with 10 ns pulse width) was focused on rotating palladium and platinum targets (Johnson-Matthey, 99.9%, and platinum crucible). Laser energies ranging from 5 to 50 mJ/pulse were employed. In experiments with neon, a 10% neutral density filter was used to reduce the laser energy. Laser-ablated metal atoms, cations, and electrons were co-deposited with nitric oxide at 0.2 to 0.3% in argon or 0.1 to 0.2% in neon onto a 10 or 4 K CsI cryogenic window at 2−4 mmol/h for 30 to 60 min. Several isotopic samples ($^{14}N^{16}O$, Matheson; $^{15}N^{16}O$, MSD Isotopes, 99%; $^{15}N^{18}O$, Isotec, 99%) and selected mixtures were used. Infrared spectra were recorded at 0.5 cm^{-1} resolution on a Nicolet 750 spectrometer with 0.1 cm^{-1} accuracy using a HgCdTe detector. Matrix samples were annealed at a range of temperatures (20−45 K, argon, and 6−12 K, neon) and subjected to broad-band photolysis by a medium-pressure mercury arc (Philips, 175 W) with the globe removed (240−580 nm). Filters were used to selectively irradiate the sample with wavelengths >470 nm and >380 nm. Experiments were repeated with trace amounts of CCl_4 (0.01−0.03%) included in the reagent gas to serve as an electron trap and alter ion yields.[26,27]

Calculations. DFT calculations were performed on the platinum and palladium nitrosyls using the Gaussian 94 program.[28] The BPW91 functional was used in all calculations, and the B3LYP functional was employed for comparison in selected cases.[29−31] The 6-311+G(d) basis set was used to represent nitrogen and oxygen,[32] and the LanL2DZ ECP basis set was used for platinum and palladium.[33,34]

Results

Absorptions observed for palladium and platinum nitrosyl products are listed in Tables 1−4. Figures 1−5 show the spectra in the nitrosyl stretching region for the palladium and platinum products in argon and neon matrices. Additional bands due to NO, $(NO)_2$, $(NO)_2^+$, $(NO)_2^-$, NO_2, and NO_2^- common to experiments with laser-ablated metal and nitric oxide are not listed in the tables.[14,15,20,21,35−37] Weak bands (A < 0.004) due to oxides of palladium and platinum including $Pd(O_2)$, $(O_2)Pd(O_2)$, OPtO, $Pt(O_2)$, and $(O_2)Pt(O_2)$ are observed in the 1100−900 cm^{-1} region.[25,38] The optimized geometries and associated harmonic frequencies of product molecules calculated using DFT are summarized in Tables 5−8, and calculated energy changes for important reactions are listed in Table 9.

Discussion

Argon Matrix Experiments. The nitrosyl chemistry is similar for nickel, palladium, and platinum. The new product bands observed when laser-ablated Pd and Pt are co-deposited with nitric oxide in argon will be identified and compared with Ni results.

MNO and $M(NO)_2$. The primary products are the neutral mononitrosyl and dinitrosyl complexes, as found in the nickel system.[18] The PdNO and PtNO absorptions decrease in intensity

10.1021/jp000796o CCC: $19.00
Published on Web 08/11/2000

TABLE 1: Infrared Absorptions (cm^{-1}) from Co-deposition of Laser-Ablated Palladium Atoms with NO in Excess Argon at 10 K

$^{14}N-^{16}O$	$^{15}N-^{16}O$ [$^{14}N^{16}O/^{15}N^{16}O$ ratio]	$^{15}N-^{18}O$ [$^{15}N^{16}O/^{15}N^{18}O$ ratio]	$^{14}N-^{16}O + ^{15}N-^{16}O$	assignment
3522.0	3454.6 [1.01951]	3373.6 [1.02400]	[a]	$Pd(NO)_2$, (sym + asym)
1921.6	1883.2 [1.02039]	[a]	1921.6, 1883.2	$PdNO^+$
1738.6	1705.0 [1.01971]	1665.2 [1.02390]	1718.5	$Pd(NO)_2$ (site)[c]
1736.2	1703.7 [1.01908]	1662.7 [1.02466]	1717.2, 1703.7	$Pd(NO)_2$ (site)
1733.8	1700.1 [1.01982]	1660.3 [1.02397]	1733.8, 1713.5, 1700.1	$Pd(NO)_2$, (asym)[c]
1723.1	1690.1 [1.01953]	[a]	[b]	$Pd_x(NO)_y$ including PdPdNO
1704.8	1675.1 [1.01773]	[a]	[b]	
1695.9	1665.4 [1.01831]	[a]	[b]	
1687.6	1660.2 [1.01650]	[a]	[b]	
1679.0	1648.9 [1.01825]	[a]	[b]	
1661.8	1632.8 [1.01776]	1593.0 [1.02498]	1661.8, 1632.8	PdNO
1572.8	1544.3 [1.01845]	1508.4 [1.02380]	1572.8, 1544.3	
1504.2	1476.6 [1.01869]	1438.7 [1.02634]	1504.2, 1476.6	Pd_2NO

[a] The band was not observed in this experiment. [b] The spectrum was too congested to observe these bands or any associated intermediates. [c] The 1738.6 cm^{-1} site favored on deposition; the 1733.8 cm^{-1} site favored on annealing.

TABLE 2: Infrared Absorptions (cm^{-1}) from Co-deposition of Laser-Ablated Palladium Atoms with NO in Excess Neon at 4 K

$^{14}N-^{16}O$	^{15}N-^{16}O [$^{14}N^{16}O/^{15}N^{16}O$ ratio]	^{15}N-^{18}O [$^{15}N^{16}O/^{15}N^{18}O$ ratio]	$^{14}N-^{16}O + ^{15}N-^{16}O$	assignment
3324.2	3265.9 [1.01785]	3180.7 [1.02679]	3324.2, 3265.9	PdNO
1924.0	1889.3 [1.01837]	1844.3 [1.02440]	1924.0, 1889.3	$PdNO^+$ (site)
1921.8	1887.1 [1.01839]	1841.4 [1.02482]	1921.8, 1887.1	$PdNO^+$
1755.5	1721.4 [1.01981]	1680.9 [1.02409]	1755.5, 1734.6, 1721.4	$Pd(NO)_2$ (site)
1753.0	1719.0 [1.01978]	1678.5 [1.02413]	1753.0, 1732.2, 1719.0	$Pd(NO)_2$
1751.3	1717.3 [1.01980]	1676.9 [1.02409]	1751.3, 1730.2, 1717.3	$Pd(NO)_2$ (site)
1680.2	1650.2 [1.01818]	1607.3 [1.02669]	1680.2, 1650.2	PdNO (site)
1676.4	1646.4 [1.01822]	1603.1 [1.02701]	1676.4, 1646.4	PdNO
1487.6	1459.1 [1.01953]	[a]	1487.6, 1459.1	$PdNO^-$

[a] The band was not observed in this experiment.

on annealing as these species are consumed in further reactions. The $Pd(NO)_2$ and $Pt(NO)_2$ absorptions, which are initially of comparable intensity to the mononitrosyl bands, show a large increase in intensity during annealing as nitric oxide molecules diffuse and combine with PdNO and PtNO in the softened matrix. These assignments are confirmed by the mixed $^{14}NO/^{15}NO$ and $^{15}N^{16}O/^{15}N^{18}O$ isotopic experiments in which the lack of intermediate peaks for the 1661.8 cm^{-1} (Pd) and 1712.6 cm^{-1} (Pt) bands indicate that only one NO subunit is involved in each case, whereas the 1:2:1 intensity patterns observed for the 1733.8 cm^{-1} (Pd) and 1763.8 cm^{-1} (Pt) absorptions indicate that two equivalent NO subunits are involved in the strong observed modes. A weak combination band at 3522.0 cm^{-1} (Pd) and 3581.5 cm^{-1} (Pt) tracked with the dinitrosyl bands on annealing. The differences $3522.0 - 1733.8 = 1788.2$ cm^{-1} and $3581.5 - 1763.8 = 1817.7$ cm^{-1} are appropriate for the symmetric nitrosyl stretching modes in $Pd(NO)_2$ and $Pt(NO)_2$, respectively.

The $^2A'$ state is found to be the ground state for both PdNO and PtNO using the BPW91 functional, and the lowest quartet state ($^4A''$) is 191−195 kJ/mol higher (Tables 5 and 6). This difference is large enough that there is no ambiguity in determining the ground states. The frequencies calculated using the BPW91 functional are 24−40 cm^{-1} higher than observed for the mononitrosyls. The very good agreement obtained with this functional and the related BP86 functional is observed in other systems and arises from a partial cancellation of errors.[39,40] These results are almost identical to those for NiNO which absorbs at 1676.6 cm^{-1} in argon, and is calculated to have a

TABLE 3: Infrared Absorptions (cm^{-1}) from Co-deposition of Laser-Ablated Platinum Atoms with NO in Excess Argon at 10 K

$^{14}N-^{16}O$	$^{15}N-^{16}O$ [$^{14}N^{16}O/^{15}N^{16}O$ ratio]	$^{15}N-^{18}O$ [$^{15}N^{16}O/^{15}N^{18}O$ ratio]	$^{14}N-^{16}O + ^{15}N-^{16}O$	assignment
3581.5	3509.4 1.02054]			$Pt(NO)_2$, (sym + asym)
2014.4	1974.0 1.02047]	[b]	2014.4, 1974.0	$PtNO^+$ (site)
2010.4	1970.1 1.02046]	[b]	2010.4, 1970.1	$PtNO^+$
1923.0	1883.2 1.02113]	[b]	1923.0, 1883.2	$PtPtNO^+$
1832.2	1794.0 1.02129]	1754.9 1.02228]	[b]	$Pt_x(NO)_y$ including PtPtNO
1829.5	1792.2 1.02081]	1752.8 1.02248]	[b]	
1827.1	1789.6 1.02095]	1751.1 1.02199]	[b]	
1813.1	1775.5 1.02118]	1737.8 1.02169]	[b]	
1804.3	1766.2 1.02157]	[a]	[b]	
1769.1	1747.4 1.01242]	1695.1 1.0308]	1769.1, 1747.4, 1733.5	$Pt(NO)_2$ (site)
1766.4	1730.9 1.02051]	1692.3 1.02281]	1766.4, 1744.5, 1730.9	$Pt(NO)_2$ (site)
1763.8	1728.2 1.02060]	1689.9 [1.02266]	1763.8, 1742.1, 1728.2	$Pt(NO)_2$, (asym)
1742.9	1709.7 1.01942]	1668.3 1.02482]	1742.9, 1723.0, 1720.1, 1668.3	$Pt_x(NO)_2$
1699.0	1665.4 1.02018]	1627.4 1.02335]	1699.0, 1680.0, 1676.2, 1665.5	$Pt_x(NO)_2$
1679.4	1647.5 1.01936]	1607.5 1.02488]	1679.4, 1647.5	PtNO (site)
1677.0	1645.2 1.01933]	1605.0 1.02505]	1677.0, 1645.2	PtNO
1522.6	1496.3 1.01758]	1455.4 1.02810]	1522.6, 1496.3	Pt_2NO
1513.8	1487.6 1.01761]	1447.1 1.02799]	1513.8, 1487.6	Pt_2NO (site)
1508.2	1482.1 1.01761]	1441.8 1.02795]	1508.2, 1482.1	Pt_2NO (site)
1505.6	1479.9 1.01737]	1439.8 1.02785]	1505.6, 1479.9	Pt_2NO (site)

[a] The band was not observed in this experiment. [b] The spectrum was too congested to observe these bands or any associated intermediates.

TABLE 4: Infrared Absorptions (cm^{-1}) from Co-deposition of Laser-Ablated Platinum Atoms with NO in Excess Neon at 4 K

$^{14}N-^{16}O$	$^{15}N-^{16}O$ [$^{14}N^{16}O/^{15}N^{16}O$ ratio]	$^{15}N-^{18}O$ [$^{15}N^{16}O/^{15}N^{18}O$ ratio]	$^{14}N-^{16}O + ^{15}N-^{16}O$	assignment
3394.8	3331.4 1.01903]	3249.2 1.02530]	3394.8, 3331.4	PtNO
2023.1	1983.3 1.02007]	1938.0 1.02337]	2023.1, 1983.3	$PtNO^+$ (site)
2019.6	1979.3 1.02036]	1934.4 1.02321]	2019.6, 1979.3	$PtNO^+$
1931.7	1893.4 1.02023]	1848.5 1.02429]	1931.7, 1893.4	$PtPtNO^+$
[a]	1743.9	1705.9 1.02228]	[a]	$Pt(NO)_2$
1776.9	1741.2 1.02050]	[a]	[a]	$Pt(NO)_2$ (site)
1716.4	1684.9 1.01870]	1642.4 1.02588]	1716.4, 1684.9	PtNO (site)
1712.6	1680.4 1.01916]	1638.9 1.02532]	1712.6, 1680.4	PtNO
1648.2	1617.9 1.01873]	1576.7 1.02613]	[a]	
1462.1	1434.7 1.01910]	1398.5 1.02588]	1461.7, 1434.7	$PtNO^-$

[a] The spectrum was too congested to observe these bands or any associated intermediates.

$^2A'$ ground state, a 1703.9 cm^{-1} nitrosyl frequency, and a bond angle of ~140°.[18,22,23] However, the less stable side-bound species Ni−(η^2-NO) is also isolated and absorbs at 1292.6 cm^{-1} in argon.[18,23] In contrast, no product band is observed near 1300 cm^{-1} in either the palladium or platinum systems, and no energy minima for the side-bound species are found using DFT.

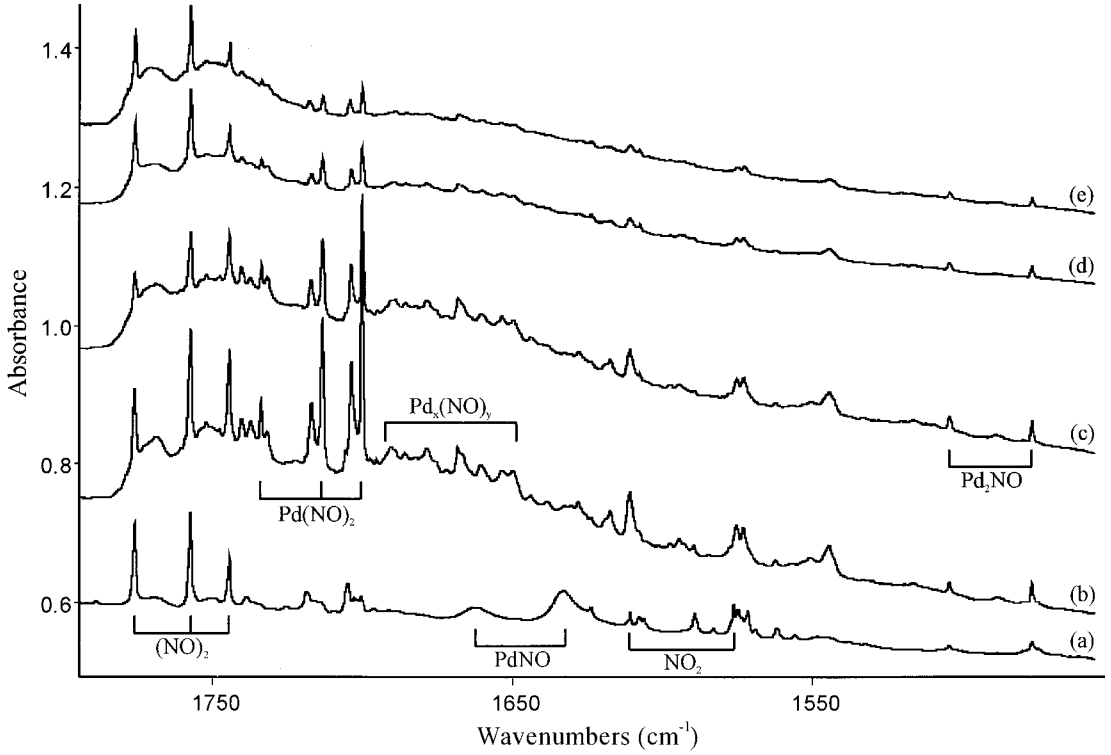

Figure 1. Infrared spectra in the 1790−1490 cm^{-1} region for laser-ablated palladium atoms with 0.08% NO + 0.2% ^{15}NO in Ar: (a) after 30 min deposition, (b) after annealing to 25 K, (c) after annealing to 30 K, (d) after 25 min photolysis, (e) after annealing to 35 K.

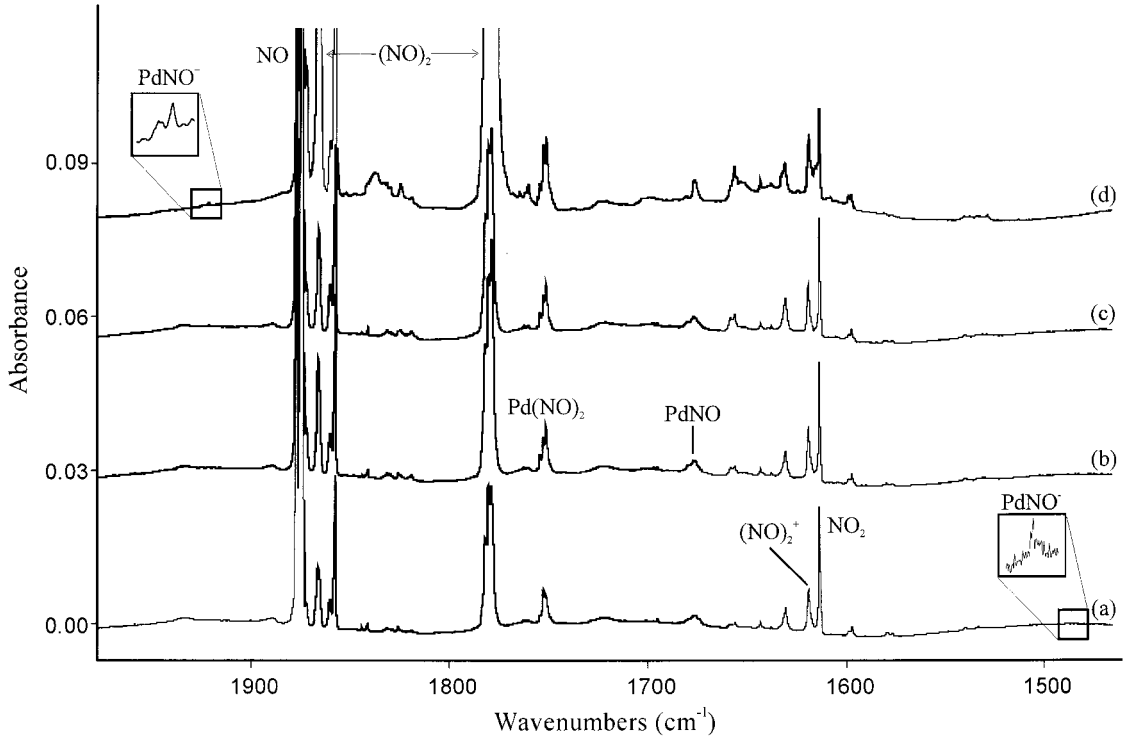

Figure 2. Infrared spectra in the 1980−1460 cm^{-1} region for laser-ablated palladium atoms with 0.1% NO in Ne: (a) after 30 min deposition, (b) after annealing to 7 K, (c) after 20 min photolysis with Hg lamp and $\lambda > 630$ nm filter, (d) after annealing to 11 K.

The calculations for PdNO and PtNO were repeated using the B3LYP functional which overestimates vibrational frequencies,[41] and the scale factors required to bring the calculated harmonic frequencies into agreement with the experimental anharmonic frequencies are in the range 0.93−0.95 (Tables 7 and 8). These calculations also support the observation that $Pd(NO)_2$ and $Pt(NO)_2$ form readily on annealing; the calculated energies strongly favor reactions 1 and 2 (Table 9). The energies calculated using the B3LYP functional are considerably lower than those for the BPW91 functional, and this is found to be the case for all reactions considered in this study. The B3LYP results are probably more accurate, considering the greater success of functionals that include Hartree−Fock exchange in calculating the binding energies of ligands in various transition metal complexes.[42]

Both dinitrosyl species are calculated to have triplet ground

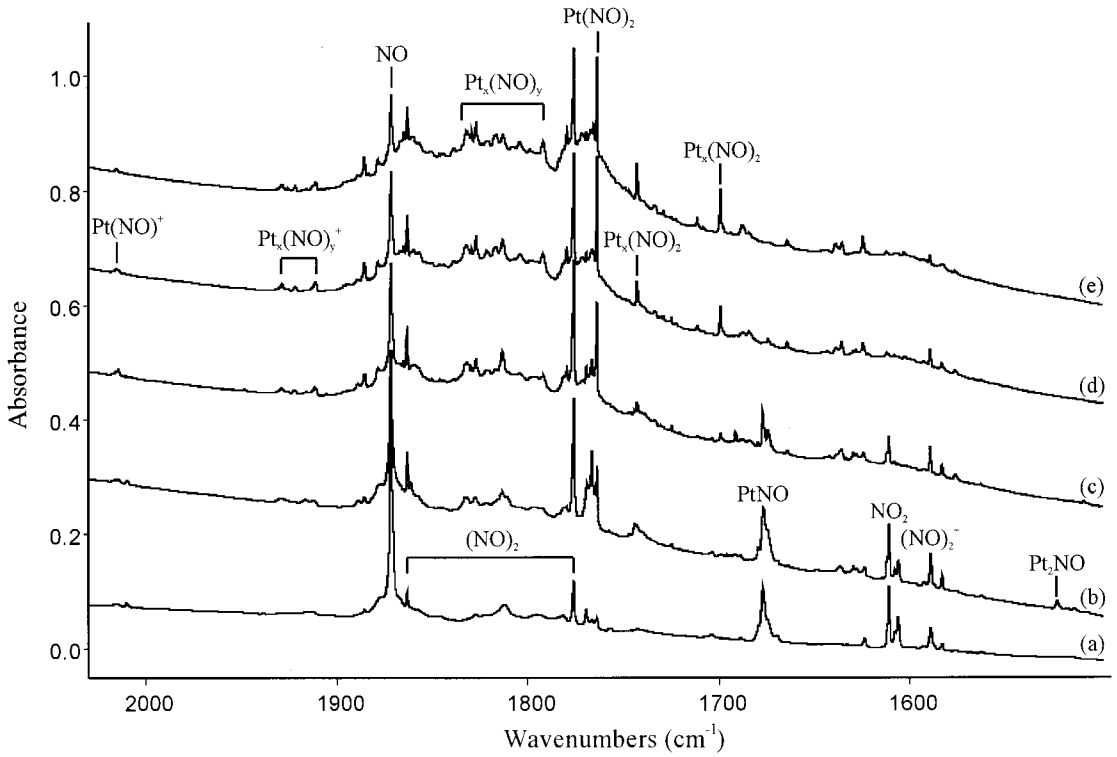

Figure 3. Infrared spectra in the 2030−1500 cm^{-1} region for laser-ablated platinum atoms with 0.3% NO in Ar: (a) after 60 min deposition, (b) after annealing to 25 K, (c) after annealing to 35 K, (d) after annealing to 40 K, (e) after annealing to 43 K.

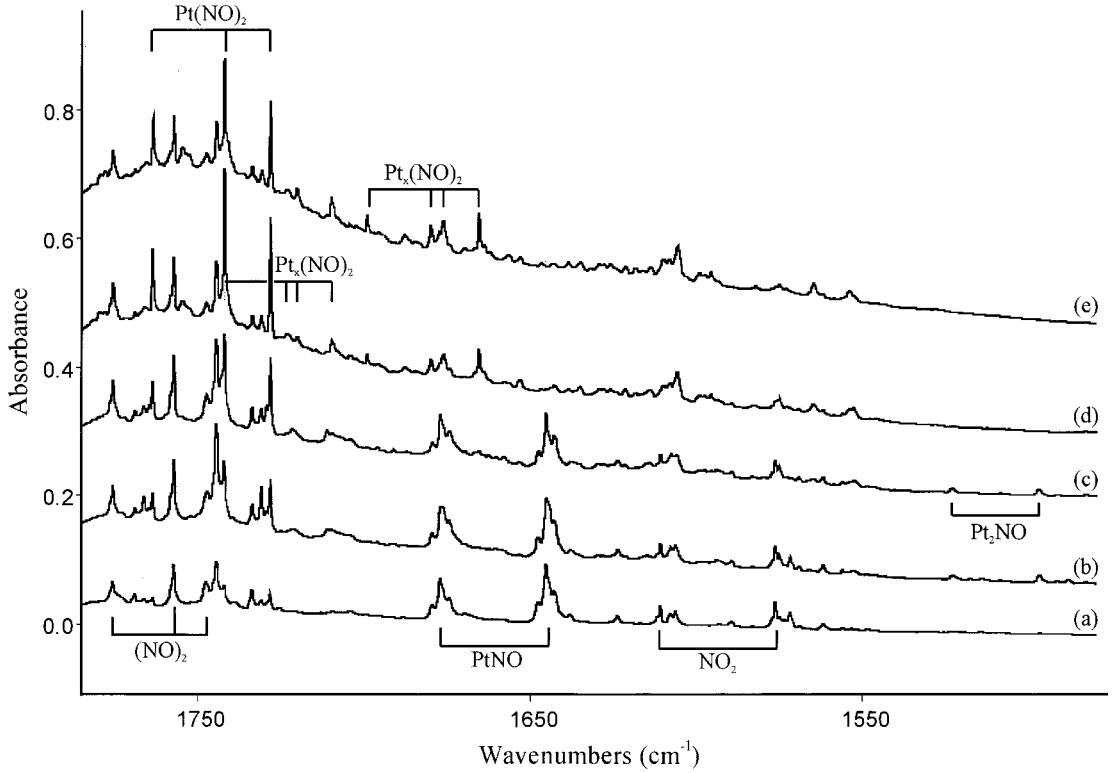

Figure 4. Infrared spectra in the 1780−1480 cm^{-1} region for laser-ablated platinum atoms with 0.15% NO + 0.2% ^{15}NO in Ar: (a) after 30 min deposition, (b) after annealing to 25 K, (c) after annealing to 30 K, (d) after annealing to 40 K, (e) after annealing to 43 K.

states and linear geometries, so only the antisymmetric N−O vibration is infrared active. The lowest singlet states are nonlinear and 50−53 kJ/mol higher in energy. In addition, the antisymmetric N−O stretch calculated for the singlet states is too low, and $^3\Sigma_g^-$ is confidently identified as the ground state for both $Pd(NO)_2$ and $Pt(NO)_2$. Almost identical results are found for $Ni(NO)_2$, which absorbs at 1749.7 cm^{-1} in argon and is calculated to have the same linear structure and ground state.[18] The symmetric and antisymmetric N−O vibrations are calculated (BPW91, Tables 5 and 6) to be 30−40 cm^{-1} higher than the deduced and observed values. The symmetric vibration is calculated to be of higher frequency for both molecules than

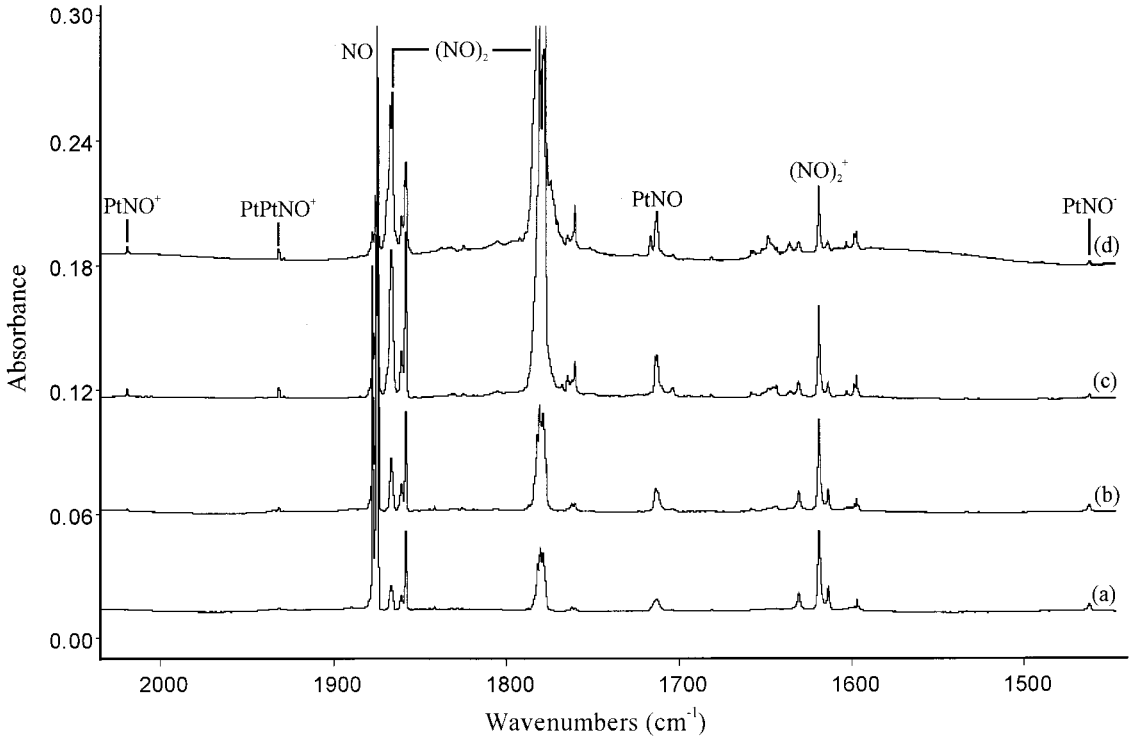

Figure 5. Infrared spectra in the 2030−1450 cm^{-1} region for laser-ablated platinum atoms with 0.19% NO in Ne: (a) after 50 min deposition, (b) after annealing to 8 K, (c) after annealing to 10 K, (d) after annealing to 12 K.

the antisymmetric mode, which is consistent with the asymmetry in the triplets observed in the mixed isotopic experiments. The intermediate components are lower than the midpoints of the pure isotopic bands by 3.5 cm^{-1} (Pd) and 3.9 cm^{-1} (Pt) which is indicative of an interaction with a higher frequency mode that has the same symmetry in the (^{14}NO)M(^{15}NO) isotopic molecule. No bands due to skeletal modes were observed for these species.

M_2NO. Other, weaker bands are observed in both metal systems. A sharp band is observed at 1504.2 cm^{-1} when palladium atoms are deposited with nitric oxide in argon which grows on first annealing but decreases in intensity on higher temperature annealing and on irradiation with a medium-pressure mercury lamp. No intermediate bands are observed in experiments using ^{14}NO/^{15}NO or ^{15}N^{16}O/^{15}N^{18}O mixtures, indicating that only one NO subunit is involved. There are two possible assignments for this band, the anionic species $PdNO^-$ or a cluster species Pd_xNO. The anion assignment is consistent with the low NO stretching frequency that has been observed for several nitrosyl anions in this laboratory.[18−20] However, anions are typically present on deposition, decrease during annealing, disappear during photolysis, and are absent when the reagent gas is doped with CCl_4 electron trap. The 1504.2 cm^{-1} band does not have these characteristics, and the assignment is rejected. The anion is not expected to be formed when relatively high laser powers are used, as the extra electron is photodetached by the radiation from the laser plume. However, anion species are observed in neon when milder ablation conditions are used, as is discussed below. The assignment of this band to a cluster species is more reasonable because higher laser powers were employed and metal atoms are expected to be more abundant in the matrix. It has been shown previously that platinum atoms are even more mobile than N_2 in argon,[43] and Pt_x clusters are certainly formed during annealing as platinum atoms diffuse through the matrix.

The simplest mononitrosyl cluster is Pd_2NO. This species has been the focus of a previous DFT study where two geometries were considered, a linear end-on geometry PdPdNO, and the bridged species Pd_2NO, the latter configuration being preferred.[9] These species have been recalculated here, and the optimized geometries and frequencies are expected to be improved with respect to those of the previous study where these parameters were calculated at the LSD level with no gradient corrections. The linear PdPdNO geometry optimized but was found to have imaginary frequencies. The calculation was repeated for a bent planar geometry and the optimized structure has all real frequencies. As in the previous work, the bridged species is lower in energy but not by a large margin. In both cases the doublet state is much lower in energy than the quartet state. The nitrosyl stretching frequency of 1540.5 cm^{-1} calculated for Pd_2NO using the BPW91 functional is 36.3 cm^{-1} higher than the 1504.2 cm^{-1} band, the same margin for error found with the $Pd(NO)_{1,2}$ and $Pt(NO)_{1,2}$ calculations. When the calculation for the doublet state of Pd_2NO is repeated using B3LYP, the NO stretching frequency is 1608.0 cm^{-1}, which requires a scale factor of 0.935 to bring it into agreement with the 1504.2 cm^{-1} band. This scale factor is comparable to those found for PdNO and $Pd(NO)_2$, and these DFT results support assignment of the 1504.2 cm^{-1} band to the bridged Pd_2NO molecule.

An analogous band is observed in the platinum system at 1522.6 cm^{-1}, which does not have any intermediate bands in either the mixed ^{14}NO/^{15}NO/Ar or ^{15}N^{16}O/^{15}N^{18}O/Ar isotope experiments indicating the participation of only one NO subunit. This band, not present initially, grows in during early annealing, but is diminished on higher temperature annealing and photolysis. This is similar to the behavior of the 1504.2 cm^{-1} band in the palladium system. The NO stretching frequency of 1555.4 cm^{-1} calculated for Pt_2NO using the BPW91 functional is 32.8 cm^{-1} higher than the observed band, the same margin of error observed in the other calculations. The B3LYP frequency of 1577.0 cm^{-1} for this molecule is too high and requires a scale factor of 0.954, comparable to those for the other B3LYP

TABLE 5: Geometries, Energies, and Frequencies Calculated for Neutral and Ionic Palladium Nitrosyls Using DFT (BPW91/LanL2DZ/6-311+G(d))

molecule	state (point group)	relative energies (kJ/mol)	$<S^2>$	geometry (Å, deg)	frequencies (cm^{-1}) [intensities (km/mol)]
PdNO	$^2A'$ (C_s)	0	0.7500	r(Pd−N): 1.890 r(N−O): 1.180 ∠PdNO: 127.4	1700.1 [750], 533.8 [6], 256.9 [4]
	$^4A''$ (C_s)	+191	3.7500	r(Pd−N): 2.002 r(N−O): 1.203 ∠PdNO: 139.5	1579.2 [996], 400.8 [10], 248.0 [4]
$PdNO^+$	$^1A'$ (C_s)	0	/	r(Pd−N): 1.864 r(N−O): 1.132 ∠PdNO: 136.0	1967.9 [431], 511.2 [20], 208.3 [3]
	$^3A'$	+183	2.0000	r(Pd−N): 2.010 r(N−O): 1.147 ∠PdNO: 145.3	1897.6 [393], 335.9 [10], 232.5 [2]
$PdNO^-$	$^1A'$ (C_s)	0	/	r(Pd−N): 1.892 r(N−O): 1.217 ∠PdNO: 122.6	1499.6 [1188], 592.5 [47], 310.3 [9]
	$^3A''$ (C_s)	+12	2.0001	r(Pd−N): 1.918 r(N−O): 1.235 ∠PdNO: 126.9	1438.7 [1032], 480.5 [34], 209.0 [5]
$Pd(NO)_2$	$^1A_1$ (C_{2v})	+50	/	r(Pd−N): 1.994 r(N−O): 1.178 ∠PdNO: 119.2 ∠NPdN: 104.4 ϕ(ONPdO): 0.0	1739.2 [414], 1648.3 [883], 594.0 [51], 432.1 [0]... 84.9 [0]
	$^3\Sigma_g^-$ ($D_{\infty h}$)	0	2.0003	r(Pd−N): 1.873 r(N−O): 1.173 ∠PdNO: 180.0 ∠NPdN: 180.0	1846.5 [0], 1774.7 [2034], 412.6 [24], 408.2 [0]...16.1 [0]×2
	^5B_g (C_{2h})	+217	6.0000	r(Pd−N): 1.979 r(N−O): 1.196 ∠PdNO: 145.1 ∠NPdN: 180.0 ϕ(ONPdO): 180.0	1698.6 [0], 1598.8 [2003], 413.2 [6], 386.3 [0] ... 61.1 [2]
PdPdNO	$^2A'$ (C_s)	+39	0.7500	r(Pd−Pd): 2.528 r(Pd−N): 1.834 r(N−O): 1.170 ∠PdPdN: 136.3 ∠PdNO: 138.0 ϕ(PdPdNO): 0.0	1763.5 [1060], 579.7 [5], 305.6 [1], 189.3 [0], 173.4 [0], 44.8 [0]
	$^4A''$ (C_s)	+158	3.7500	r(Pd−Pd): 2.515 r(Pd−N): 1.979 r(N−O): 1.184 ∠PdPdN: 161.4 ∠PdNO: 151.3 ϕ(PdPdNO): 0.0	1721.1 [852], 380.9 [1], 233.7 [9], 187.2 [0], 37.3 [1], −202.4 [5]
$(Pd)_2NO$	$^2A'$ (C_s)	0	0.7500	r(Pd−Pd): 2.642 r(Pd−N): 1.978 r(N−O): 1.205 ∠$(Pd)_2$NO: 138.1	1540.5 [676], 506.9 [6], 444.4 [6], 261.5 [4], 183.3 [0], 158.2 [0]
	$^4A''$	+168	3.7500	r(Pd−Pd): 2.958 r(Pd−N): 2.016 r(N−O): 1.217 ∠$(Pd)_2$NO: 146.2	1459.9 [761], 351.7 [11], 271.8 [7], 260.8 [2], 153.6 [0], 80.9 [0]
$PdPdNO^+$	$^1A'$	0	/	r(Pd−Pd): 2.688 r(Pd−N): 1.855 r(N−O): 1.144 ∠PdPdN: 118.3 ∠PdNO: 137.8 ϕ(PdPdNO): 0.0	1897.4 [732], 529.6 [7], 263.8 [3], 146.9 [1], 96.3 [0], 28.9 [0]
	$^3A'$	57	2.0000	r(Pd−Pd): 2.591 r(Pd−N): 1.905 r(N−O): 1.145 ∠PdPdN: 99.0 ∠PdNO: 142.1 ϕ(PdPdNO): 0.0	1871.8 [874], 448.2 [6], 260.8 [2], 172.6 [2], 71.1 [0], 64.8 [0]

calculations in this work. These calculations support the assignment of the 1522.6 cm^{-1} band to the bridged Pt_2NO molecule. However, the alternative PtPtNO geometry is calculated to be 95 kJ/mol *lower* in energy than the bridged Pt_2NO geometry (BPW91). This species is found to be linear, unlike the palladium analogue. The NO stretching frequency of 1864.4 cm^{-1} calculated for linear PtPtNO is a few tens of wavenumbers higher than a series of peaks observed in the range 1830−1792 cm^{-1} that grow in during annealing. The B3LYP frequency of 1945.8 cm^{-1} for this molecule requires a scale factor of 0.939

TABLE 6: Geometries, Energies, and Frequencies Calculated for Neutral and Ionic Platinum Nitrosyls Using DFT (BPW91/LanL2DZ/6-311+G(d))

molecule	state (point group)	relative energies (kJ/mol)	$<S^2>$	geometry (Å, deg)	frequencies (cm^{-1}) [intensities (km/mol)]
PtNO	$^2A'$ (C_s)	0	0.7500	r(Pt−N): 1.814 r(N−O): 1.177 ∠PdNO: 134.8	1717.6 [698], 610.6 [3], 309.4 [5]
	$^4A''$ (C_s)	+195	3.7500	r(Pt−N): 1.957 r(N−O): 1.198 ∠PtNO: 139.8	1614.9 [632], 446.3 [5], 262.1 [10]
$PtNO^+$	$^1\Sigma^+$ ($C_{\infty v}$)	0	/	r(Pt−N): 1.754 r(N−O): 1.130 ∠PdNO: 180.0	2043.8 [447], 568.5 [16], 255.7 [6]×2
	$^3A'$ (C_s)	+154	2.0000	r(Pt−N): 1.888 r(N−O): 1.144 ∠PdNO: 141.4	1865.2 [674], 523.2 [20], 334.0 [8]
$PtNO^-$	$^1A'$ (C_s)	0	/	r(Pt−N): 1.865 r(N−O): 1.221 ∠PtNO: 122.1	1471.7 [818], 674.5 [16], 350.7 [2]
	$^3A''$ (C_s)	+85	2.0000	r(Pt−N): 1.858 r(N−O): 1.233 ∠PtNO: 141.0	1469.5 [816], 540.1 [48], 278.7 [11]
$Pt(NO)_2$	$^1A'$ (C_s)	+53	/	r(Pt−N): 1.887 r(N−O): 1.178 ∠PtNO: 137.1 ∠NPtN: 152.7 ϕ(ONPtN): 28.5	1769.3 [95], 1700.0 [1547], 541.6 [14], 454.5 [6], 422.9 [1]..0.55.0 [0]
	$^3\Sigma_g^-$ ($D_{\infty h}$)	0	2.0002	r(Pt−N): 1.826 r(N−O): 1.175 ∠PtNO: 180.0 ∠NPtN: 180.0	1870.3 [0], 1794.3 [1612], 520.1 [0], 448.2 [20] ... 49.8 [0]×2
PtPtNO	$^2\Sigma^+$ ($C_{\infty v}$)	0	0.7500	r(Pt−Pt): 2.407 r(Pt−N): 1.784 r(N−O): 1.164 ∠PtPtN: 180.0 ∠PtNO: 180.0	1864.4 [1069], 551.0 [1], 401.7 [3]×2, 202.4 [2], 40.3 [0]×2
	$^4A''$	+142	3.7500	r(Pt−Pt): 2.439 r(Pt−N): 1.909 r(N−O): 1.180 ∠PtPtN: 159.8 ∠PtNO: 140.7 ϕ(PtPtNO): 180.0	−48.1 [0], 53.6 [1], 185.0 [0], 276.6 [7], 475.8 [34], 1712.7 [922]
Pt_2NO	$^2A'$	+95	0.7501	r(Pt−Pt): 2.577 r(Pt−N): 1.973 r(N−O): 1.198 ∠$(Pt)_2$NO: 147.1	1555.4 [637], 573.5 [23], 468.2 [4], 311.2 [8], 187.2 [0], 164.3 [0]
	$^4A'$	+160	3.7500	r(Pt−Pt): 2.627 r(Pt−N): 2.009 r(N−O): 1.193 ∠$(Pt)_2$NO: 146.6	1571.5 [675], 524.0 [0], 440.7 [5], 301.4 [7], 182.7 [1], 140.1 [0]
$PtPtNO^+$	$^1\Sigma^+$	+12	/	r(Pt−Pt): 2.407 r(Pt−N): 1.789 r(N−O): 1.138 ∠PtPtN: 180.0 ∠PtNO: 180.0	1985.1 [1038], 539.9 [29], 395.6 [0]×2, 189.2 [0], 42.2 [1]×2
	?	0	2.0000	r(Pt−Pt): 2.453 r(Pt−N): 1.802 r(N−O): 1.134 ∠PtPtN: 180.0 ∠PtNO: 180.0	1999.8 [1048], 517.7 [29], 376.6 [0]×2, 174.0 [0], 28.7 [1]×2

to bring it into agreement with the highest frequency band in the 1830−1792 cm^{-1} region. It is reasonable to assume that one of these peaks is probably due to PtPtNO. The other bands in this range could be due to higher Pt_nNO clusters in which NO is bound end-on. An attempt was made to calculate Pt_3NO with NO in a terminal site, but these calculations had convergence problems. The fact that the less stable bridged geometry is also present indicates that the matrix annealing reaction(s) are formed are under kinetic rather than thermodynamic control. When the less stable product is formed, it does not have sufficient energy at such low temperatures to rearrange to the more stable geometry.

There are two routes by which the cluster products could form, either addition of a platinum atom to PtNO, or the combination of Pt_2 with NO. Perhaps one of these mechanisms kinetically favors the higher energy geometry due to the relative orientations of the precursors when they encounter each other. The energy changes for these reactions have been calculated (reactions 3−10, Table 9), and all are found to be favorable. The same reasoning must apply to the palladium system, and the less stable PdPdNO product is expected to be present in the matrix in addition to the bridged Pd_2NO geometry. A series of bands grows during annealing in the range 1723−1672 cm^{-1}, analogous to the bands in the platinum system. The NO

TABLE 7: Geometries, Energies, and Frequencies Calculated for Selected Neutral and Ionic Palladium Nitrosyls Using DFT (B3LYP/LanL2DZ/6-311+G(d))

molecule (ground state) [relative energy, kJ/mol]	$<S^2>$	geometry (Å, deg)	frequencies (cm^{-1}) [intensities (km/mol)]	ν(NO) scale factors	
				argon	neon
PdNO ($^2A'$)	0.7502	r(Pd−N): 1.927 r(N−O): 1.167 ∠PdNO: 128.7	1786.8 [731], 480.0 [7], 227.8 [4]	0.9305	0.9382
$PdNO^+$ ($^1A'$)	/	r(Pd−N): 1.875 r(N−O): 1.116 ∠PdNO: 132.7	2062.2 [562], 507.1 [31], 210.2 [4]	/	0.9319
$PdNO^-$ ($^1A'$) [+12]	/	r(Pd−N): 1.898 r(N−O): 1.205 ∠PdNO: 122.1	1556.0 [1477], 586.1 [54], 308.8 [15	/	0.9560
$PdNO^-$ ($^3A''$) [0]	2.0006	r(Pd−N): 1.954 r(N−O): 1.226 ∠PdNO: 124.6	1484.6 [1401], 444.6 [36], 197.8 [7]	/	1.0020
$Pd(NO)_2$ ($^3\Sigma_g^-$) [0]	2.0053	r(Pd−N): 1.878 r(N−O): 1.161 ∠PdNO: 180.0 ∠NPdN: 180.0	1911.1 [0], 1830.0 [2737], 419.6 [71], 401.7 [0]..0.28.1 [1]×2	0.9474	0.9577
$Pd(NO)_2$ ($^1A_1$) [+50]	/	r(Pd−N): 2.005 r(N−O): 1.164 ∠PdNO: 118.9 ∠NPdN: 101.1 ϕ(ONPdO): 0.0	1825.7 [478], 1708.7 [1127], 588.9 [54], 439.0 [2]..0.120.5 [0]	/	/
Pd_2NO ($^2A'$)	0.7504	r(Pd−Pd): 2.533 r(Pd−N): 2.052 r(N−O): 1.167 ∠$(Pd)_2$NO: 139.6	1608.0 [699], 502.2 [10], 422.7 [6], 237.0 [8], 176.3 [0], 145.1 [0]	0.9354	/
PdPdNO ($^2A'$)	0.7504	r(Pd−Pd): 2.590 r(Pd−N): 1.856 r(N−O): 1.159 ∠PdPdN: 122.9 ∠PdNO: 133.6 ϕ(PdPdNO): 0.0	1812.2 [1328], 559.9 [12], 304.6 [1], 171.5 [1], 125.8 [0], 36.9 [0]	~0.95	/
$PdPdNO^+$ ($^1A'$) [0]	/	r(Pd−Pd): 2.712 r(Pd−N): 1.862 r(N−O): 1.127 ∠PdPdN: 115.5 ∠PdNO: 134.8 ϕ(PdPdNO): 0.0	1988.9 [902], 533.5 [15], 278.0 [3], 143.4 [2], 102.2 [1], 32.6 [0]	/	/

stretching frequency of 1763.5 cm^{-1} calculated for PdPdNO using the BPW91 functional is 40 cm^{-1} higher than the highest frequency band in that range, the same difference as was observed for the platinum bands, which supports the tentative assignment of one of these bands to PdPdNO. The frequency calculated using B3LYP is 1812.2 cm^{-1}, which requires a scale factor of 0.951 to agree with the 1723.1 cm^{-1} band, and the assignment of a band in this range to PdPdNO is supported. The other bands in this range could be due to higher cluster products in which NO is bound end-on. Unfortunately the spectra are too congested to be able to determine whether intermediate components are present in the mixed isotope experiments, but none are expected. The large difference in the relative stability of the bridged and end-on bound nitrosyls of Pt_2 and Pd_2 is consistent with a detailed theoretical study of the interaction between these metal dimers and a hydrogen molecule,[6] and it follows that NO would preferentially bind at one platinum atom. The bridged Pt_2NO molecule is a stable structure; however, the experimental data indicate that molecules formed in this geometry are unable to rearrange to the energetically favorable end-bound form at such low temperatures. The electronic structure of Pd_2 is different from that of Pt_2 in that the metal−metal σ bonding orbital is higher in energy and is now the HOMO. An incoming NO molecule therefore interacts with Pd more strongly at the center of the dimer rather than at one end. The lower energy of Pd_2NO relative to PdPdNO is consistent with this, although the energy difference is only 39 kJ/mol, perhaps because the end-bound species is bent with the NO group closer to the center of the metal dimer. Linear PdPdNO optimized but gave imaginary frequencies, and conversely an initially bent PtPtNO geometry became linear during the geometry optimization.

No such species were reported in the nickel−nitrosyl system, but reexamination of the argon spectra reveals weak, sharp bands at 1503.8, 1802.6, 1808.4, and 1813.5 cm^{-1} that grow on moderate annealing, and do not exhibit significant intermediate peaks in either the $^{15}N^{16}O/^{15}N^{18}O$ or $^{14}N^{16}O/^{15}N^{16}O$ mixed isotopic sample experiments.[18] These were listed as $Ni_x(NO)$, denoting uncharacterized cluster species, but in light of the above discussion they might be appropriate for the N−O stretching vibration in Ni_2NO and NiNiNO, with the additional bands in the upper region being due to higher end-on bound $Ni_x(NO)$ clusters or matrix sites. DFT calculations using the BP86 functional predict $^2A'$ ground states for both the nonplanar bridged geometry Ni_2NO and the nearly linear NiNiNO geometries, the latter being 3 kJ/mol higher in energy. The N−O stretching frequencies of 1520.9 and 1807.5 cm^{-1} calculated for these geometries are in excellent agreement with the observed bands. In addition, the calculated $^{14}N^{16}O/^{15}N^{16}O$ and $^{15}N^{16}O/^{15}N^{18}O$ isotopic ratios of 1.0199 and 1.02488 (Ni_2NO), and 1.0214 and 1.0222 (NiNiNO) are also in very good agreement with the respective experimental values of 1.0200, 1.0233, 1.0207, and 1.0224 for the bands at 1503.8 and 1802.6 cm^{-1}, giving further support to these tentative assignments.

MNO^+. Absorptions due to cation products in argon are observed for both metals. In the palladium system, a sharp band

TABLE 8: Geometries, Energies, and Frequencies Calculated for Selected Neutral and Ionic Platinum Nitrosyls Using DFT (B3LYP/LanL2DZ/6-311+G(d))

molecule (ground state) [relative energy, kJ/mol]	$<S^2>$	geometry (Å, deg)	frequencies (cm^{-1}) [intensities (km/mol)]	ν(NO) scale factors	
				argon	neon
PtNO ($^2A'$)	0.7501	r(Pt−N): 1.823 r(N−O): 1.1648 ∠PtNO: 133.4	1782.9 [821], 602.9 [4], 304.7 [2]	0.9406	0.9605
$PtNO^+$ ($^1\Sigma^+$)	/	r(Pt−N): 1.764 r(N−O): 1.115 ∠PtNO: 180.0	2129.7 [631], 557.3 [26], 217.4 [5]×2	/	0.9483
$PtNO^-$ ($^1A'$)	/	r(Pt−N): 1.857 r(N−O): 1.210 ∠PtNO: 121.7	1528.1 [1020], 691.7 [17], 359.7 [4]	/	0.9565
$Pt(NO)_2$ ($^1A_1$) [+69]	/	r(Pt−N): 1.880 r(N−O): 1.164 ∠PtNO: 139.0 ∠NPtN: 155.3	1857.1 [99], 1767.9 [2018], 546.3 [10], 436.2 [1]...47.6 [0]	/	/
$Pt(NO)_2$ ($^3\Sigma_g$-) [0]	2.0038	r(Pt−N): 1.826 r(N−O): 1.164 ∠PtNO: 180.0 ∠NPtN: 180.0	1928.4 [0], 1849.0 [2025], 520.0 [0], 444.3 [55]... 54.9 [0]×2	0.9539	/
Pt_2NO ($^2A'$)	0.7504	r(Pt−Pt): 2.591 r(Pt−N): 1.971 r(N−O): 1.191 ∠$(Pt)_2$NO: 143.7	1577.0 [858], 583.1 [13], 483.9 [6], 324.7 [3], 189.5 [0], 161.2 [0]	0.9655	/
PtPtNO ($^2\Sigma^+$)	0.7500	r(Pt−Pt): 2.449 r(Pt−N): 1.774 r(N−O): 1.147 ∠PtPtN: 180.0 ∠PtNO: 180.0	1945.8 [1331], 569.8 [3], 409.1 [4]×2, 190.9 [6], 22.6 [0]×2	∼0.94	/
$PtPtNO^+$ ($^1\Sigma_g$+) [0]	/	r(Pt−Pt): 2.491 r(Pt−N): 1.773 r(N−O): 1.121 ∠PtPtN: 180.0 ∠PtNO: 180.0	2080.2 [1331], 565.3 [33], 385.6 [0]×2, 148.7 [3], 34.8 [1]×2	0.9237	0.9286
$PtPtNO^+$ ($^3A'$) [+7]	2.0000	r(Pt−Pt): 2.550 r(Pt−N): 1.795 r(N−O): 1.122 ∠PtPtN: 147.9 ∠PtNO: 162.8 ϕ(PtPtNO): 0.0	2069.4 [920], 550.1 [6], 377.3 [5], 291.7 [0], 152.7 [1], 45.4 [3]	0.9285	0.9335

TABLE 9: Energy Changes (kJ/mol) for Reactions Calculated Using the BPW91 and B3LYP Functionals[a]

reaction	ΔE (BPW91)	ΔE (B3LYP)	reaction
1	−222	−186	PdNO ($^2A'$) + NO ($^2\Pi$) → $Pd(NO)_2$ ($^3\Sigma_g$-)
2	−161	−108	PtNO ($^2A'$) + NO ($^2\Pi$) → $Pt(NO)_2$ ($^3\Sigma_g$-)
3	−148	−94	Pd (^1S) + PdNO ($^2A'$) → PdPdNO ($^2A'$)
4	−187	−146	Pd (^1S) + PdNO ($^2A'$) → Pd_2NO ($^2A'$)
5	−208	−126	Pd_2 ($^3\Sigma_u$+) + NO ($^2\Pi$) → PdPdNO ($^2A'$)
6	−247	−178	Pd_2 ($^3\Sigma_u$+) + NO ($^2\Pi$) → Pd_2NO ($^2A'$)
7	−321	−256	Pt (^3D) + PtNO ($^2A'$) → PtPtNO ($^2\Sigma^+$)
8	−226	−175	Pt (^3D) + PtNO ($^2A'$) → Pt_2NO ($^2A'$)
9	−288	−211	Pt_2 ($^3\Sigma_g$-) + NO ($^2\Pi$) → PtPtNO ($^2\Sigma^+$)
10	−193	−130	Pt_2 ($^3\Sigma_g$-) + NO ($^2\Pi$) → Pt_2NO ($^2A'$)

[a] Including zero point energy corrections but not BSSE effects.

is observed at 1921.6 cm^{-1} when CCl_4 is present, but was not observed otherwise. This suggests that the band is due to a cationic species. No intermediate band was observed in the NO/^{15}NO mixed isotopic experiment, and $PdNO^+$ is the most obvious assignment. The lowest singlet state is much lower in energy than the lowest triplet state with both functionals, so there is no ambiguity in deciding the ground state. The BPW91 N−O stretching frequency for this state is 1967.9 cm^{-1}, which is 46.3 cm^{-1} higher than the observed band, and the same frequency calculated with the B3LYP functional is 2062.2 cm^{-1}, which requires a scale factor of 0.932. These results support assignment of the 1921.6 cm^{-1} band to $PdNO^+$, by comparison with the level of accuracy found for other molecules in this work. However, $PdPdNO^+$ must also be considered. The singlet state is calculated to be significantly lower in energy than the triplet state, so only the frequencies calculated for the former need to be considered. The BPW91 N−O stretching frequency for this species is 1897.3 cm^{-1}, which is 24.3 cm^{-1} *lower* than the observed band, and the B3LYP frequency is 1988.9 cm^{-1}, which requires a scale factor of 0.966. This is not as good a fit as was found for $PdNO^+$. In fact, the calculations suggest that the N−O stretching frequency of $PdPdNO^+$ should be lower than this, probably obscured by absorptions due to NO or $(NO)_2$, if it is present at all. The 1921.6 cm^{-1} band is therefore assigned to $PdNO^+$.

In the platinum system, a sharp weak band at 2014.7 cm^{-1}

grows in slightly during early annealing in argon, but decreases at higher temperatures. No intermediate band is observed in either the $^{14}NO/^{15}NO$ or $^{15}N^{16}O/^{15}N^{18}O$ mixed isotope experiments, which shows that only one NO unit is involved. When the experiment is repeated with trace quantities of CCl_4 in the reagent gas, the yield of these bands is increased by a factor of 4 with respect to the yield of PtNO, which is indicative of a positively charged species.[44] The most likely assignment for these bands is to the molecular ion $PtNO^+$. This is supported by the fact that this species is observed in a neon matrix only 5 cm^{-1} higher in frequency (discussed below) and by the DFT calculations. The N−O stretching frequency calculated for $PtNO^+$ using the BPW91 functional is 29.4 cm^{-1} higher than the experimental value, and the frequency calculated using B3LYP is higher and requires a scale factor of 0.946. The results for $PtNO^+$ are almost identical to those for $NiNO^+$, which is also calculated to have a $^1\Sigma^+$ ground state and absorbs at 2001.9 cm^{-1} in neon.[18] The lower frequency observed for $PdNO^+$ is attributed to its bent geometry.

Another group of seven bands in the range 1931−1911 cm^{-1} is present on deposition, increases on early annealing, but then decreases on annealing to higher temperatures. These bands are analogous to the bands in the range 1830−1792 cm^{-1} assigned to neutral metal cluster species. No intermediates are observed when the experiment was repeated with a $^{14}NO/^{15}NO$ mixture. With CCl_4 additive and lower laser power, a single broad band was observed at 1923.4 cm^{-1} that exhibited the same annealing behavior and no intermediate bands in the $^{14}NO/^{15}NO$ mixed isotope experiment. The intensity of this band is enhanced, which suggests that this is also due to a cation. $PtNO^+$ has already been identified, and a reasonable assignment for this band is to the charged cluster species $PtPtNO^+$. The range of bands observed in the experiment without CCl_4 would then be due to larger $Pt_n(NO)^+$ clusters. The singlet and triplet states of $PtPtNO^+$ are close in energy; the triplet state is only 12 kJ/mol lower than the singlet when the BPW91 functional is used, and the singlet state is 7 kJ/mol lower than the triplet using the B3LYP functional. Clearly, both states must be considered. The quintet state is calculated to be much higher in energy with both functionals and is ignored. The ion is optimized to a linear geometry for both the singlet and triplet states using the BPW91 functional, with very similar N−O stretching frequencies that are 61.9 cm^{-1} (singlet) and 76.6 cm^{-1} (triplet) higher than the band at 1923.2 cm^{-1}. The B3LYP frequencies of 2080.2 cm^{-1} (singlet) and 2069.4 cm^{-1} (triplet) are high and require scale factors of 0.925 and 0.929, respectively. These calculations are in qualitative agreement with experiment.

$Pt_x(NO)_2$. Sharp bands grow in at 1742.9 and 1699.0 cm^{-1} during annealing in the platinum−argon system that exhibit 1:1:1:1 quartets in the $NO/^{15}NO$ and $^{15}NO/^{15}N^{18}O$ mixed isotope experiments, indicating the participation of two inequivalent NO groups. Several possible structures were calculated but none give frequencies compatible with these observations, and no identification can be made.

Neon Matrix Experiments. Significantly lower laser energies were used to generate metal atoms when experiments were repeated in neon. This allows molecular ions to be trapped which are destroyed due to irradiation by the laser plume at the metal surface when higher energies are used.

MNO and $M(NO)_2$. The primary products in both the platinum and palladium systems are the mono and dinitrosyls MNO and $M(NO)_2$, blue shifted in frequency relative to the argon matrix values, which is typical for the vibrational frequencies of species trapped in neon vs argon.[18,45] This difference is similar for the NO stretching modes of PdNO and $Pd(NO)_2$ which are 14.6 and 19.2 cm^{-1} higher in neon than in argon, which are slightly larger than the matrix differences, 3.5 and 12.3 cm^{-1}, for NiNO and $Ni(NO)_2$, respectively.[18] However, the PtNO absorption in neon is 35.6 cm^{-1} higher than the argon value, although the $^{14}NO/^{15}NO$ and $^{15}N^{16}O/^{15}N^{18}O$ isotopic ratios are almost identical in neon and argon. No absorption due to $Pt(^{14}NO)_2$ is readily apparent in the neon experiment, but two bands that are unique to the platinum system are observed in the experiment using ^{15}NO at 1743.9 and 1741.2 cm^{-1} just below the strong absorption due to $^{15}(NO)_2$. If it is assumed that these bands are due to $Pt(^{15}NO)_2$ in two different matrix sites and that the isotopic ratio is the same for this molecule in argon (as is the case for PtNO), then the ^{14}NO counterparts for these absorptions would be 1779.8 and 1777.1 cm^{-1}, respectively. The higher frequency band is obscured by the strong $^{14}(NO)_2$ absorption, but a weak band is observed at 1776.9 cm^{-1} in the ^{14}NO experiment, which supports this interpretation. If the same $^{15}N^{16}O/^{15}N^{18}O$ ratio for $Pt(NO)_2$ in argon is applied to the 1743.9 and 1741.2 cm^{-1} bands, then the $^{15}N^{18}O$ counterparts for these are expected at 1705.3 and 1702.6 cm^{-1}. The lower band is obscured by $(^{15}N^{18}O)_2$, but a band that grows in on annealing is observed at 1705.9 cm^{-1} and is suitable for assignment to the higher frequency matrix site of $Pt(^{15}N^{18}O)_2$. If this assignment to $Pt(NO)_2$ in neon is correct, then the neon−argon shift is 13.2 cm^{-1}, comparable to those observed for PdNO and $Pd(NO)_2$ but lower than the anomalous matrix shift for PtNO.

The N−O overtones are observed for PdNO and PtNO at 3324.2 cm^{-1} and 3394.8 cm^{-1} in neon. The differences $2 \times \nu(NO) - 2\nu(NO)$ are 31.4 and 30.4 cm^{-1} for PdNO and PtNO and 28.7 cm^{-1} for NiNO.[18] The difference between the first overtone and twice the fundamental frequency for NO in solid neon[29] is 28.1 cm^{-1}, which shows that the nitrosyl vibrations in PdNO and PtNO are only slightly more anharmonic than NO itself.

$M(NO)^{+,-}$. In addition to these neutral products, the molecular ions $PdNO^+$, $PdNO^-$, $PtNO^+$, and $PtNO^-$ are also observed. The presence of only one NO group is demonstrated from the absence of intermediate bands in either mixed isotope experiment. The anions are present initially, but decrease rapidly in intensity on annealing. They are also very sensitive to photolysis, being diminished when irradiated with light of $\lambda < 370$ nm, and completely destroyed when exposed to unfiltered light from the Hg lamp. The cations are more resilient to irradiation, being destroyed by full arc photolysis but not with 370−580 nm light. The cations show a marked growth on lower annealing, decreasing slightly at the highest annealing temperatures. When the gas sample was doped with CCl_4, the anion bands were diminished and the cation bands were enhanced, which supports these assignments.[18,22] The anions and cations have low and high NO stretching frequencies, respectively, owing to the greater and lesser population of the π^* orbitals of the ligand in these ions with respect to the neutral molecules.

The DFT calculations for these ions are of similar quality to those for the neutral molecules. Both cations have singlet ground states with triplet states much higher in energy. $PtNO^+$ and $PdNO^+$ were observed in neon at frequencies 4.9 and 2.4 cm^{-1} higher than the argon matrix values, and the DFT results were discussed above. In the case of $PtNO^-$, the $^3A''$ state is 85 kJ/mol higher than the $^1A'$ state, and there is no doubt that the latter is the ground state. The N−O stretching frequency of $PtNO^-$ calculated for this state is 9.6 cm^{-1} higher than the band assigned to this species, and the B3LYP frequency scale factor

is 0.957, which supports this assignment. It is less clear in the case of $PdNO^-$ because the $^1A'$ state is calculated to be just 12 kJ/mol lower than the $^3A''$ state using the BPW91 functional. This is too close to determine which is ground state using the energies alone; the frequencies must also be considered. The N−O stretching frequency for the $^1A'$ state of 1499.6 cm^{-1} is 12 cm^{-1} higher than the experimental value of 1487.6 cm^{-1}, comparable to the result for the $^1A'$ state of $PtNO^-$, and the frequency for the $^3A''$ state is 48.9 cm^{-1} *lower* than this value, which would indicate that the singlet state is correct. The results of the B3LYP calculations are much clearer on this point. Although the $^3A''$ state is calculated to be 12 kJ/mol lower in energy than the $^1A'$ state with this functional, the N−O stretching frequency of the triplet state is marginally *lower* than the observed frequency and would have to be scaled by 1.0020. This would be qualitatively different to the other species reported in this study, and the $^3A''$ state may be rejected. By contrast, the N−O stretching frequency for the $^1A'$ state is higher than the experimental value and a scale factor of 0.956 is required. The same ground state is also predicted for $NiNO^-$ which absorbs at 1454.7 cm^{-1} in neon.[18]

Nitrosyl Chemistry. The nitrosyl stretching frequencies of the observed species are within the typical ranges for nitrosyl complexes.[46] The 2-fold bridge species Ni_2NO, Pd_2NO, and Pt_2NO absorb in the 1480−1545 cm^{-1} range observed for analogous nitrosyl complexes, and the bent mononitrosyls NiNO, PdNO, and PtNO absorb in the 1525−1700 cm^{-1} range expected for bent NO groups. The bands assigned to NiNiNO, PdPdNO, and PtPtNO are in the 1600−2000 cm^{-1} range expected for linear on-top nitrosyl complexes, although the DFT calculations for NiNiNO and PdPdNO gave slightly nonlinear geometries. The adsorption of nitric oxide on these metal surfaces is predominantly molecular in nature, and molecules in both bridged and on-top sites have been reported on palladium and platinum. On the Pt(110) surface, bands are observed at 1610−1630 cm^{-1} and assigned to 2-fold bridge sites.[13] At high coverage, the bridged species disappears and is replaced by an on-top species with a frequency of ∼1760 cm^{-1}. In both cases the NO molecule is thought to be perpendicular to the surface, based on other experimental and theoretical work.[7] The difference between these frequencies, 150−130 cm^{-1}, is comparable to the 155 cm^{-1} difference between PtNO and Pt_2NO observed in this work.

Similar results are found for NO on Pd(111), where bands observed at 1734−1758 cm^{-1} and 1586−1620 cm^{-1} are assigned to NO at a top site and 2-fold bridge site, the frequencies depending on the coverage.[11] The results of DFT calculations for NO chemisorbed on palladium clusters indicate that the molecule is perpendicular to the surface.[5] The difference of ∼143 cm^{-1} between these sites is comparable to the 157 cm^{-1} difference between PdNO and Pd_2NO observed in this work. This indicates that results for NO bound to one- and two-metal atoms can reproduce the frequency differences observed for different adsorption sites on the respective metal surfaces, though the DFT calculations show that these species have bent NO units whereas the surface species are normal to the surface. On Ni(100), bands of increasing frequency in the range 1300−1700 cm^{-1} are observed as the coverage is increased. These bands are attributed to NO bound to progressively lower coordination sites.[47] A band at 1669 cm^{-1} assigned to NO on a top site is very close to the band at 1680.1 cm^{-1} assigned to NiNO in argon.[18]

The chemistry of supported metal catalysts is also of interest. For example, platinum-metal catalysts including Pt/ZSM-5 and Pd/ZSM-5 foster the selective reduction of nitric oxide by hydrocarbons in excess oxygen, Pt/ZSM-5 being the most active.[48] When NO is adsorbed on this catalyst, a band is observed at 1909 cm^{-1} that has been attributed to NO bound to a partially oxidized metal atom.[48] This is consistent with the present work in which both $PtNO^+$ and PtNO have been observed; 1909 cm^{-1} falls between the NO stretching frequencies for these species. The NO stretching frequencies (in neon) for the cation, neutral, and anion platinum and palladium mononitrosyls are plotted against charge in Figure 6, and both are found to be nearly linear. Using the best fit line for the platinum data and the observed frequency of 1909 cm^{-1}, the charge on the partially oxidized platinum in ZSM-5 is estimated to be +0.6. Similarly, infrared bands observed at 1803, 1754, and 1655 cm^{-1} for NO adsorbed on Pd/Al_2O_3 have been assigned to $[Pd]-NO^+$, [Pd]−NO, and $[Pd]-NO^-$.[49] The plot in Figure 6 cannot be used to estimate charges since the supported palladium crystallites consist of many metal atoms, but it does suggest that the actual range of charges in this series is less than +1 to −1. The same linear relationship is found for the nickel mononitrosyls,[18] and the N−O stretching frequency of 1892 cm^{-1} measured[50] for nitric oxide on $Ni^{II}Y$ suggests an effective charge of +0.7.

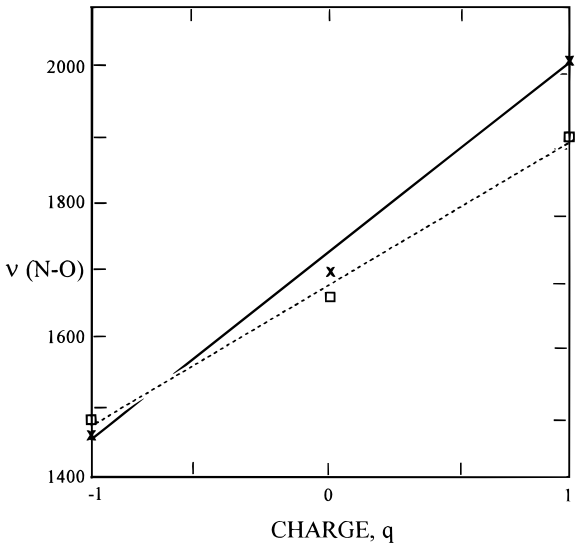

Figure 6. Plot of nitrosyl stretching frequencies vs charge in the $Pt(NO)^{+,0,-}$ and $Pd(NO)^{+,0,-}$ series.

Conclusions

Products of the reaction between laser ablated palladium and platinum atoms and nitric oxide have been isolated in neon and argon matrices and characterized by infrared spectroscopy and DFT calculations. $Pd(NO)_{1,2}$ and $Pt(NO)_{1,2}$ are found to be the dominant products with metal cluster secondary products in argon matrices where higher laser powers were used. The milder conditions used in neon experiments allowed the ionic species $Pd(NO)^+$, $Pt(NO)^+$, $Pd(NO)^-$, and $Pt(NO)^-$ to be observed. An additional charged species is observed in the platinum argon and neon systems and is tentatively assigned to $PtPtNO^+$. The DFT calculations prove to be very effective in reproducing the NO stretching frequencies of the various products, the BPW91 functional consistently giving frequencies within 2% of the observed values. The B3LYP frequencies are invariably too high, but scale down to the experimental values in a consistent manner that compliments the BPW91 results. The results for the isolated species correlate well with the known surface chemistry of these metals, and the linear relationship between

the charge and the NO stretching frequencies in $Pt(NO)^{+,0,-}$ allows the charge on partially oxidized platinum atoms in Pt/ZSM-5 to be estimated. The same relationship between charge and frequency is found in the $Pd(NO)^{+,0,-}$ series.

The results for palladium and platinum are very similar to those for the nickel nitrosyls reported previously[18,23] with the exception of $Ni-(\eta^2\text{-NO})$, for which no palladium or platinum counterparts are observed.

Acknowledgment. We gratefully acknowledge N.S.F. support under grant CHE 97-00116.

References and Notes

(1) Wang, H.; Carter, E. A. *J. Phys. Chem.* **1992**, *96*, 1197.
(2) Matsumoto, H.; Tanabe, S. *J. Phys. Chem.* **1995**, *99*, 6951.
(3) Harada, M.; Dexpert, H. *J. Phys. Chem.* **1996**, *100*, 565.
(4) Rochefort, A.; Fournier, R. *J. Phys. Chem.* **1996**, *100*, 13506.
(5) Jigato, M. P.; Somasundram, K.; Termath, V.; Handy, N. C.; King, D. A. *Surf. Sci.* **1997**, *380*, 83.
(6) Cui, Q.; Musaev, D. G.; Morokuma, K. *J. Chem. Phys.* **1998**, *108*, 8418.
(7) Ge, Q.; King, D. A. *Chem. Phys. Lett.* **1998**, *285*, 15.
(8) Cui, Q.; Musaev, D. G.; Morokuma, K. *J. Phys. Chem. A* **1998**, *102*, 6373.
(9) Zacarias, A. G.; Castro, M.; Tour, J. M.; Seminario, J. M. *J. Phys. Chem. A* **1999**, *103*, 7692.
(10) Agrawal, V. K.; Trenary, M. *Surf. Sci.* **1991**, *259*, 116.
(11) Chen, P. J.; Goodman, D. W. *Surf. Sci.* **1993**, *297*, L93. Xu, X.; Chen, P.; Goodman, D. W. *J. Phys. Chem.* **1994**, *98*, 9242.
(12) Wang, H.; Tobin, R. G.; DiMaggio, C. L.; Fisher, G. B.; Lambert, D. K. *J. Chem. Phys.* **1997**, *107*, 9569.
(13) Brown, W. A.; Sharma, R. K.; King, D. A. *J. Phys. Chem. B* **1998**, *102*, 5303.
(14) Zhou, M. F.; Andrews, L. *J. Phys. Chem. A* **1999**, *103*, 478 (V+NO).
(15) Andrews, L.; Zhou, M. F.; Ball, D. W. *J. Phys. Chem. A* **1998**, *102*, 10041 (Mn+NO).
(16) Zhou, M. F.; Andrews, L. *J. Phys. Chem. A* **1998**, *102*, 7452 (Cr+NO), Zhou, M. F.; Andrews, L. *J. Phys. Chem. A* **1998**, *102*, 10025 (Nb, Ta+NO).
(17) Kushto, G. P.; Zhou, M. F.; Andrews, L.; Bauschlicher, C. W., Jr. *J. Phys. Chem. A*, **1999**, *103*, 1115 (Sc, Ti).
(18) Zhou, M.; Andrews, L. *J. Phys. Chem. A* **2000**, *104*, 3915. (Ni).
(19) Zhou, M.; Andrews, L. *J. Phys. Chem. A* **2000**, *104*, 2618. (Cu).
(20) Zhou, M.; Andrews, L. *J. Phys. Chem. A* **1998**, *102*, 7452 (Cr).
(21) Zhou, M.; Andrews, L. *J. Phys. Chem. A* **1999**, *103*, 4167 (Mo, W).
(22) Ruschel, G. K.; Nemetz, T. M.; Ball, D. W. *J. Mol. Struct.* **1996**, *384*, 101.
(23) Krim, L.; Manceron, L.; Alikhani, M. E. *J. Phys. Chem. A* **1999**, *103*, 2592.
(24) Burkholder, T. R.; Andrews, L. *J. Chem. Phys.* **1991**, *95*, 8697.
(25) Bare, W. D.; Citra, A.; Chertihin, G. V.; Andrews, L. *J. Phys. Chem. A* **1999**, *103*, 5456.
(26) Zhou, M.; Andrews, L. *J. Chem. Phys.* **1999**, *111*, 10370.
(27) Zhou, M.; Andrews, L. *J. Am. Chem. Soc.* **1999**, *121*, 9171.
(28) Frisch, M. J.; Trucks, G. W.; Schlegel, H. B.; Gill, P. M. W.; Johnson, B. G.; Robb, M. A.; Cheeseman, J. R.; Keith, T.; Petersson, G. A.; Montgomery, J. A.; Raghavachari, K.; Al-Laham, M. A.; Zakrzewski, V. G.; Ortiz, J. V.; Foresman, J. B.; Cioslowski, J.; Stefanov, B. B.; Nanayakkara, A.; Challacombe, M.; Peng, C. Y.; Ayala, P. Y.; Chen, W.; Wong, M. W.; Andres, J. L.; Replogle, E. S.; Gomperts, R.; Martin, R. L.; Fox, D. J.; Binkley, J. S.; Defrees, D. J.; Baker, J.; Stewart, J. P.; Head-Gordon, M.; Gonzalez, C.; Pople, J. A. *Gaussian 94, Revision B.1* Gaussian, Inc.: Pittsburgh, PA, 1995.
(29) Becke, A. D. *Phys. Rev. A* **1988**, *38*, 3098.
(30) Perdew, J. P.; Wang, Y. *Phys. Rev. B* **1992**, *45*, 13244.
(31) Becke, A. D. *J. Chem. Phys.* **1993**, *98*, 5648.
(32) Krishnan, R.; Binkley, J. S.; Seeger, R.; Pople, J. A. *J. Chem. Phys.* **1980**, *72*, 650.
(33) Wadt, W. R.; Hay, P. J. *J. Chem. Phys.* **1985**, *82*, 284.
(34) Hay, P. J.; Wadt, W. R. *J. Chem. Phys.* **1985**, *82*, 299.
(35) Jacox, M. E.; Thompson, W. E. *J. Chem. Phys.* **1990**, *93*, 7609.
(36) Andrews, L.; Zhou, M. F.; Willson, S. P.; Kushto, G. P.; Snis, A.; Panas, I. *J. Chem. Phys.* **1998**, *109*, 177.
(37) Andrews, L.; Zhou, M. F. *J. Chem. Phys.* **1999**, *111*, 6036.
(38) Huber, H.; Klotzbücher, W.; Ozin, G. A.; Vander Voet, A. *Can. J. Chem.* **1973**, *31*, 2722.
(39) Andrews, L.; Bare, W. D.; Chertihin, G. V. *J. Phys. Chem. A*, **1997**, *101*, 8417.
(40) Chertihin, G. V.; Andrews, L.; Bauschlicher, C. W., Jr. *J. Am. Chem. Soc.* **1998**, *120*, 3205.
(41) Choi, C. H.; Kertesz, M. *J. Phys. Chem.* **1996**, *100*, 16530.
(42) Siegbahn, P. E. M.; Blomberg, M. R. A. *Annu. Rev. Phys. Chem.* **1999**, *50*, 221.
(43) Green, D. W.; Thomas, J.; Gruen, D. M. *J. Chem. Phys.* **1973**, *58*, 5453.
(44) Zhou, M.; Andrews, L. *J. Phys. Chem. A* **1999**, *103*, 7773 (Rh+CO).
(45) Jacox, M. *Chem. Phys.* **1994**, *189*, 149.
(46) Root, T. W.; Fisher, G. B.; Schmidt, L. D. *J. Chem. Phys.* **1986**, *85*, 4679.
(47) Avouris, Ph.; DiNardo, N. J.; Demuth, J. E. *J. Chem. Phys.* **1984**, *80*, 491.
(48) Xin, M.; Hwang, I. C.; Woo, S. I. *J. Phys. Chem. B* **1997**, *101*, 9005.
(49) Almusaiteer, K.; Chuang, S. S. C. *J. Catal.* **1999**, *184*, 189.
(50) Naccache, C.; Taarit, Y. B. *J. Chem. Soc., Faraday. Trans 2*, **1973**, *69*, 1475.